



# Ameliorating cold stress in a hot climate: Effect of Winter Storm Uri on residents of subsidized housing neighborhoods

Xiaoyu Li<sup>a</sup>, Yue Zhang<sup>a</sup>, Dongying Li<sup>a</sup>, Yangyang Xu<sup>b</sup>, Robert D. Brown<sup>a,\*</sup>

<sup>a</sup> Department of Landscape Architecture and Urban Planning, Texas A&M University, College Station, TX, 77843, USA

<sup>b</sup> Department of Atmospheric Sciences, College of Geosciences, Texas A&M University, College Station, TX, 77843, USA

## ARTICLE INFO

### Keywords:

Winter storm  
Subsidized housing  
Cold stress  
Clothing insulation  
Windbreak

## ABSTRACT

Global climate change has increased the risks of extreme weather-related disasters, leading to severe public health burdens. In February 2021, Winter Storm Uri brought severe cold to southern United States and caused unprecedented health and safety concerns. Residents in subsidized rental housing were among the most vulnerable to cold stress during such a cold storm. However, existing research on the assessment and mitigation of cold stress in underserved neighborhoods in warmer climate zones is limited, which results in the negligence of cold event preparedness and mitigation policies. Therefore, this study aims to assess the micrometeorological conditions and human cold stress in subsidized housing neighborhoods during the 2021 Winter Storm and determine the extent to which cold mitigation windbreak designs are effective in reducing cold stress. Field measurements, ENVI-met simulations, and biometeorological calculations were conducted to reconstruct the microclimate conditions and cold stress during the storm, and three cold-mitigation windbreak designs with varying foliage densities were evaluated. Results showed that the conditions were categorized as “extreme cold stress” for the majority of the day, but especially during nighttime. Areas close to the buildings were generally warmer, and the wind-blocking effects of a building decreased as the distance to the building increased. A moderately dense-foliage windbreak was the most effective in reducing wind speed and improving thermal comfort. Intentional environmental modifications to alter wind velocity and disaster relief programs that provide emergency clothing supplies during power outage may be beneficial to these underserved communities.

## 1. Introduction

The record-setting Winter Storm Uri hit the United States in the week of February 13–17, 2021, bringing extremely low temperatures that led to destructive circumstances. Texas cities were among the hardest hit due to multilevel unpreparedness, particularly regarding the power outage that ensued. Approximately 4.5 million homes and businesses in Texas lost power, and 69% of residents experienced blackouts lasting an average of 42 h [1]. At least 210 Texans died due to the winter storm, with the major cause being hypothermia [2] due to home temperatures dropping dramatically during the blackout, even to levels similar to the outdoor temperatures [3]. Other anecdotally-reported health issues included shivering, muscle stiffness, and loss of consciousness [3], which are typical cold stress symptoms.

Although this winter storm may appear to be a one-time event, broad vulnerability of southern cities to cold stress presents an urgent challenge to society. Global climate change has increased the intensity and

frequency of extreme weather events, leading to severe public health burdens. Although increasing research attention has been paid to flooding and heat events, cold surges are also related to heart disease, respiratory distress, hypothermia, and increased mortality [4–6]. Temperature-related mortality models account that the impacts of extreme weather conditions depend on latitude and climatic zone; specifically, populations in warmer regions are more vulnerable during extreme cold temperatures, and those in cooler regions are more vulnerable during heat extremes [7,8]. Although it may sound contradictory, this pattern can be explained by the level of preparedness and adaptation capacities across the geographic span—southern cities are more prepared for and adapted to hot weather, but ill-prepared for cold weather. Thus, the lack of existing research of southern cities such as in Texas on extreme cold stress, insufficient preparedness, and failure to develop mitigation policies are of serious concerns.

More concerning is that the impacts of environmental disasters such as cold storms are not evenly distributed [9]; disadvantaged populations such as those living in subsidized housing are disproportionately

\* Corresponding author. Landscape Architecture & Urban Planning, 3137 TAMU, Texas A&M University, College Station, TX, 77843-3137, USA.

E-mail address: [rbrown@arch.tamu.edu](mailto:rbrown@arch.tamu.edu) (R.D. Brown).

<https://doi.org/10.1016/j.buildenv.2021.108646>

Received 15 September 2021; Received in revised form 29 November 2021; Accepted 1 December 2021

Available online 4 December 2021

0360-1323/© 2021 Elsevier Ltd. All rights reserved.

### Nomenclature

|                  |   |
|------------------|---|
| ANOVA            | Analysis of variance  |
| C                | Convective heat flow  |
| COMFA            | COMfort Formula (COMFA) energy budget model   |
| Conv             | Sensible convective heat exchange ( $W/m^2$ )   |
| $E_D$            | Latent heat flow to evaporate water diffusing through the skin (imperceptible perspiration) |
| $E_{Re}$         | Sum of heat flows for heating and humidifying inspired air                                  |
| $E_{Sw}$         | Heat flow due to evaporation of sweat   |
| Evap             | Evaporative heat loss ( $W/m^2$ )   |
| LAD <sub>m</sub> | Max leaf area density ( $m^2/m^3$ )   |
| M                | Metabolic energy for heating the body ( $W/m^2$ )   |
| $M_{PET}$        | Metabolic rate  |
| NOAA             | National Oceanic and Atmospheric Administration   |
| PET              | Physiological equivalent temperature ( $^{\circ}C$ )  |
| R                | Net radiation of the body   |
| $R^2$            | Coefficient of determination  |
| Rabs             | Absorbed solar and terrestrial radiation ( $W/m^2$ )  |
| RMSE             | Root Mean Square Error  |
| S                | Storage heat flow for heating or cooling the body mass                                      |
| TRemitted        | Emitted terrestrial radiation ( $W/m^2$ )   |
| W                | Physical work output  |

affected by weather-related stressors. Such disaster disparities are often connected to outdated housing infrastructure and inefficient management and maintenance. Due to a lack of funding, units in subsidized housing neighborhoods were built with limits on facilities like heating, ventilation, and air conditioning. Then, maintenance is often deferred because expenses increase as the building ages, leaving many residents with poor insulation and inefficient heating and cooling systems [10]. Moreover, these neighborhoods are often populated disproportionately by minority households and located in poor and segregated communities. The socioeconomic disadvantages exacerbate disaster impacts, as these residents have fewer behavioral adaptation strategies on account of their limited financial resources and weaker social support [11]. Residents may lack warm clothes, which may not be considered necessities in warm climate zones. In addition, residents in public housing report worse health conditions than other city residents and often suffer from preexisting health conditions [12,13], rendering them even more susceptible to severe symptoms and comorbidity during a cold event. However, while prior studies have reported concerning indoor and outdoor heat exposures for residents of public housing neighborhoods [14,15], to our knowledge, no study has investigated cold stress in subsidized housing neighborhoods, much less evaluated mitigation strategies. Concrete research evidence regarding cold stress severity during extreme cold events and corresponding mitigation strategies in these most-disadvantaged neighborhoods can lessen the future impacts of similar disasters and promote equity in disaster response and preparedness.

To address this gap, we selected three subsidized housing neighborhoods as study sites, aiming to assess the micrometeorological conditions and cold stress during Winter Storm Uri and identify mitigation strategies through simulations performed in the ENVI-met model, a numerical model that simulates the effect of changes in the environment on the local microclimate, and two different human energy balance models Physiological Equivalent Temperature (PET) and COMFA. The specific objectives of this study are to: 1) assess the micrometeorological conditions and human cold stress in subsidized housing neighborhoods during the winter storm, and 2) determine the effectiveness of certain mitigation designs in reducing cold stress in affected areas.

### 1.1. The built environment and human thermal comfort

In the last few decades, studies assessing urban thermal comfort have been carried out in various built environmental settings such as streets, parks, residential areas, and schools [16], the majority of which evaluated pedestrians' thermal comfort on urban streets. It is well-documented that the effects of a street canyon are closely related to vegetation, building, and ground materials, as well as the site's morphological attributes as expressed by sky view factors, street orientation, and aspect ratio [17–19]. Some studies conducted in urban parks [20] and urban squares and university campuses [21] have examined the thermal sensations experienced among urban populations in different climate zones. Other studies have targeted the open spaces of residential areas in order to assess the influences of various design elements on site microclimate conditions, understand residents' thermal comfort, and seek practical design guidelines for outdoor spaces [22, 23]. Still other settings in which human thermal conditions have been evaluated include courtyards [24], waterfront areas [25], tourist spots [26], and open-air transportation hubs [27].

Table 1 summarizes the seasons, type of thermal comfort, and study settings. Most studies focused on the hot condition of summer, except Oliveira et al. [25] that discussed thermal comfort in spring and late winter. In addition, a few studies focused on both hot and cold conditions in summer and winter [16,17,19,22,23,26–28]. In terms of mitigation of cold stress, wind speed and solar radiation were considered to be the primary modifiable factors for cold stress [17,18,23,25,27,28].

**Table 1**  
Season, thermal comfort, and location that previous studies focused on.

| Related studies             | Season                                | Related thermal comfort | Setting                                    |
|-----------------------------|---------------------------------------|-------------------------|--|
| [16] Lau Et al. (2015)      | spring/summer/autumn/winter           | cold/hot                | Street canyon, Square, Courtyard           |
| [17] Andreou et al. (2013)  | summer/winter                         | cold/hot                | Street canyon                              |
| [18] Gulyás et al. (2006)   | Summer                                | hot                     | Urban street                               |
| [19] Johansson (2006)       | summer/winter                         | cold/hot                | Urban street canyon                        |
| [20] Lai et al. (2014)      | summer/winter                         | cold/hot                | Park                                       |
| [21] Yang et al. (2013)     | Summer                                | hot                     | Parks, squares, streets, university campus |
| [22] Lai et al. (2014)      | summer/autumn                         | cold/hot/neutral        | Residential community                      |
| [23] Mi et al. (2020)       | spring/summer/winter                  | cold/hot/neutral        | Residential community                      |
| [24] Bakar et al. (2016)    | N/A (similar weather in four seasons) | hot                     | Courtyard                                  |
| [25] Oliveira et al. (2007) | late winter/spring                    | cold/hot/neutral        | Riverside                                  |
| [26] Xi et al. (2020)       | summer/winter                         | cold/hot/neutral        | Urban square, riverside square             |
| [27] Piselli et al. (2018)  | spring/Summer/Autumn/Winter           | cold/hot/neutral        | Urban transit area                         |
| [29] de Dear et al. (1991)  | summer                                | hot                     | Buildings (indoor)                         |
| [30] Wong et al. (2002)     | summer                                | hot                     | Public housing (indoor)                    |
| [31] Sosa et al. (2018)     | summer                                | hot                     | Social housing neighborhoods (outdoor)     |
| [32] Mahmoud et al. (2019)  | summer                                | hot                     | Low-income residential community           |
| [33] Paramita et al. (2018) | summer                                | hot                     | Low-cost apartment (for low income)        |
| [34] Lau Et al. (2019)      | summer                                | hot                     | Mixed urban area                           |
| [35] Gabbe et al. (2020)    | summer                                | hot                     | Subsidized housing                         |

Some studies further pointed out that the effect of wind speed was more obvious under colder conditions [25,28]. Moreover, Mi et al. [23] and Piselli et al. [27] indicated trees and building structures could be the environmental intervention to reduce wind speed thus mitigate cold stress.

### 1.2. Outdoor thermal comfort in public housing neighborhoods

However, while many studies listed above have examined human thermal conditions in residential areas or urban buildings, research specifically on residents' outdoor thermal comfort in public housing neighborhoods is limited. Most studies in low-income or subsidized housing neighborhoods have explored indoor thermal conditions in terms of occupants' living environments, adaptability to environmental stressors, and energy consumption [29–31]; only a few have assessed outdoor thermal environments in subsidized housing neighborhoods. Mahmoud et al. and Paramita et al. discussed the impacts of building forms and configurations on residents' thermal comfort in public housing neighborhoods [32,33]. Krebs et al. investigated the cooling effects of green roofs on a public housing project in Brazil [36]. Lau et al. and Huang et al. evaluated summer microclimate conditions, human heat stress, and outdoor activities in public housing estates [15,34]. Additionally, at the neighborhood scale, Gabbe and Pierce examined the extreme heat vulnerability of residents in subsidized housing in California [35]. Moreover, unlike research in other urban contexts (e.g., street canyons, urban parks, and university campuses) that considered thermal conditions across all four seasons [20,23,28], existing studies on subsidized housing neighborhoods have only examined summertime heat stress. Therefore, the cold stress experienced by residents in public housing neighborhoods and its relation to thermal environment remains undocumented and requires research attention.

### 1.3. Methods for examining urban microclimate and outdoor thermal comfort

Three approaches are commonly used to examine urban microclimates and assess human thermal comfort: *in situ* measurements, field surveys, and three-dimensional (3D) simulations. These approaches can be applied individually or in combination. *In situ* measurements seek to quantify built environment characteristics (e.g., sky view factors) and meteorological conditions. These measurements are often used as inputs in thermal comfort models to compute thermal comfort indices such as the physiological equivalent temperature (PET) [37], which are mostly based on six main parameters: air temperature, radiation, humidity, wind speed, clothing thermal resistance, and activity [38]. Field surveys use questionnaires or in-person interviews to collect information about personal characteristics and human thermal experiences. These data can be used separately or as validation for thermal comfort models. 3D simulations exploit modeling software to simulate on-site microclimate environments and compute human thermal perceptions.

A review of recent literature indicated that study methods based on these three primary approaches can be divided into five main types of workflows:

- I. Studies that use *in situ* measurements to collect meteorological data and calculate thermal indices (e.g., PET) to assess thermal comfort [19,39].
- II. Studies that conduct 3D simulations using ENVI-met [40] and RayMan [18] to simulate outdoor thermal conditions and compute human thermal comfort levels.
- III. Studies that combine *in situ* measurements with microclimate simulation using ENVI-met [41,42] or RayMan [43].
- IV. Studies that utilize *in situ* measurements and surveys in parallel [28,44,45].
- V. Studies that integrate all three methods: field measurements, surveys, and simulations [27,46].

As 3D simulation gains popularity in microclimate modeling, ENVI-met has been widely applied to simulate urban thermal environments [47]. It allows for the adjustment of built environmental characteristics such as building density and material palette, ground surfaces, and vegetation coverage [48,49]. A number of studies have used ENVI-met to evaluate thermal conditions in residential areas and reveal the impact of building layout on thermal comfort [32,33,50]. Studies using ENVI-met usually feature three pivotal steps: modeling, validation, and scenario simulation [47].

Overall, there is a lack of studies investigating thermal comfort in the built environments of subsidized neighborhoods. Moreover, no study to date has investigated cold stress in such neighborhoods, nor the relationships between clothing thermal insulation and human cold stress in that context. In addition, most simulations have focused on heat mitigation scenarios, thus evidence regarding built environment design strategies to mitigate cold stress is also lacking. Ultimately, these significant knowledge gaps hinder progress in enhancing disaster adaptability through environmental planning and policy, leaving behind society's most vulnerable populations. Particularly, in warmer climate zones such as Texas, extreme cold conditions are rare and difficult to assess and require a study workflow that leverages the strengths of *in situ* measurements and model simulation, as in the present study.

## 2. Materials and methods

The research has four major steps (Fig. 1). The first step is the model validation, in which data through in-situ measurement was used to adjust and validate the ENVI-met model. Then in the next step, the previous literature and COMFA energy fluxes were considered to determine the key factor influencing the microclimate condition, thus three scenarios (single-row windbreak with various LAD<sub>m</sub>) were determined. And the original scenario (Feb. 15) with those three scenarios (after intervention) were simulated in the validated ENVI-met model. In the third step, the simulated micrometeorological results were collected and analyzed. And the last step is to calculate the biometeorological indices using the meteorological data acquired from step III. Detailed descriptions of material and methods are in the following sections.

### 2.1. Study areas

Study sites were chosen from subsidized housing neighborhoods in Bryan–College Station, Texas, which was among the hardest-hit areas during the 2021 winter storm and reached a record-low daily high temperature of  $-7^{\circ}\text{C}$ . Neighborhoods across the area were subject to rolling power outages, with each outage lasting from half an hour to several hours or even a full day. Subsidized housing neighborhoods suffered more due to outdated infrastructure conditions and social vulnerabilities.

All subsidized housing neighborhoods in Bryan–College Station have between 0 and 250 units and were classified as small (0–49 units), medium (50–99 units) and large (100–250 units). We randomly selected one neighborhood from each size category, yielding a collection of three neighborhoods: Haven Apartments (Site I) and Lulac Oak Hill Apartments (Site II) and Forest Park Apartments (Site III) (Fig. 2). These three residential areas are funded through the Low-Income Housing Tax Credit (LIHTC) program, which provides subsidized rental housing to seniors, disabled persons, and eligible low-income families. Residency in Haven and Forest Park Apartment is mostly restricted to households earning less than 50% or 60% of the Area Median Income (AMI), while Lulac Oak Hill is specifically for low-income elderly residents who can live independently.

### 2.2. *In situ* micrometeorological measurement

In the wake of Winter Storm Uri, the research team conducted field micrometeorological measurements in the three neighborhoods for

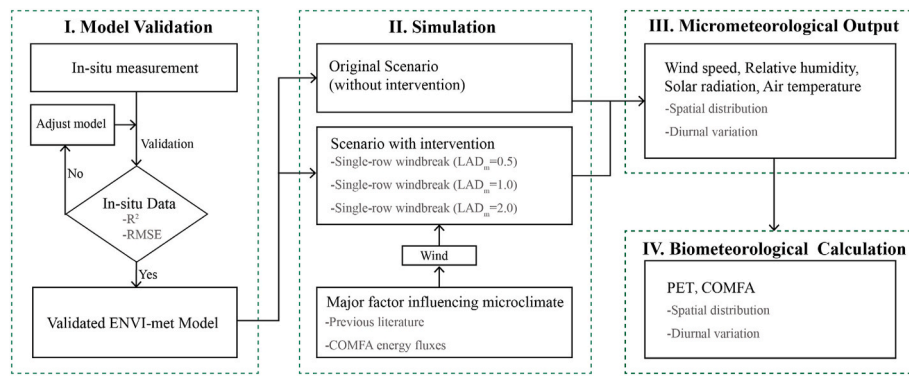


Fig. 1. Framework of the study.

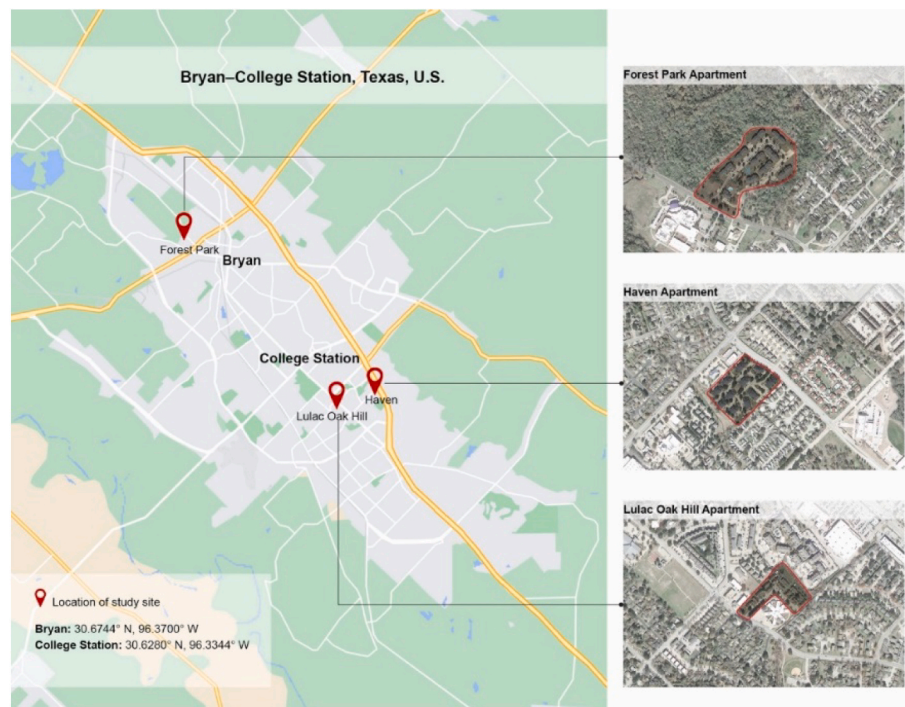


Fig. 2. Location of the study sites in Bryan-College Station, TX, U.S.

validation and triangulation purposes. As the extremely low temperature did not reoccur, measurements were taken on cool spring days with wind speed, wind direction, and solar radiation conditions that closely resembled those during the storm. This decision was made based on the established knowledge that air temperature and humidity are often insensitive to micro-level environmental features while wind conditions and radiation during a snowy day are the factors that most strongly impact human cold stress [51]. Thus, measurements were taken in March when the air temperature was lower than 20 °C, wind speed was higher than 6.7 m/s, and wind direction was from the north and north-northeast.

Data were collected for a total of 60 min in each neighborhood, with a duration of 1–2 min at each location at a temporal sampling rate of 10 s using a MaxiMet GMX501 Compact Weather Station (Gill Instruments, Hampshire, UK) placed 1.5 m above the ground. The GMX501 Compact weather station integrated the measurement of wind speed & direction, pressure, air temperature, relative humidity. The data could be reported every 1 s to every 1 h (set to be every 10s in the study) and the resolution is 0.01 for wind speed, 1° for wind direction, 0.1 for temperature [52].

For each neighborhood, we sampled one location out in the open

space away from any building as the base point and then another eight locations surrounding an apartment building (Five points located in the downwind direction, other 3 points located in the other three directions). As the pretest showed that the microclimate conditions change sharply in the downwind direction of the building [53], we included D1-D5 as five sample locations with 5 m space between each point, and D1 was 5 m away from the building wall (Fig. 3). Whereas one location was used for the other three directions 5 m away from the wall of the building. F1 point located on the upwind direction of the building, L1 and R1 respectively located on the west and south side of the building, all of them were 5 m away from the wall. Measurements taken consisted of air temperature (°C), wind speed (m/s), wind direction (degrees), and relative humidity (%) (Fig. 3).

To capture a wider spectrum of conditions and validate the accuracy of the simulation performed by ENVI-met, we also used micrometeorological data obtained in these same neighborhoods during the summertime, namely in June 2020 and July 2020, when the average daily air temperature was above 24 °C and highest temperature was above 32 °C. Measurements again consisted of air temperature (°C), wind speed (m/s), wind direction (degrees), and relative humidity (%).

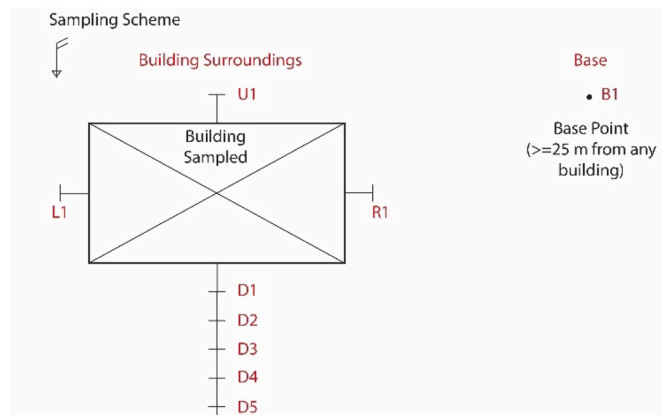


Fig. 3. Sampling scheme.

### 2.3. Micrometeorological simulation using ENVI-met

We simulated the microclimate conditions during Winter Storm Uri using ENVI-met, a high-resolution microclimate modeling software package. The biggest advantage of ENVI-met over the other models is that it can perform more comprehensive calculations and provide higher resolution output. In contrast, STEVE focus on points of interest of urban setting, which can predict air temperature at the particular point more accurately, but it cannot calculate other urban climate-related variables like wind speed [54]. Therefore, it is better suited for research for specific points and the surrounding environment. Regarding the differences between ENVI-met and TRNSYS, although TRNSYS provides very accurate MRT calculation, the processing of plants is very rough, because it does not support complicated Geometric models [55]. Compared to UMG, ENVI-met has a finer resolution. Although UMG can predict air temperature more accurately, the simplification and assumptions of the model prevent it from capturing site-specific microclimate effects [56]. For this study, high-resolution data of planar distribution, thermal comfort calculation, and hourly temperature resolution are all very important. Therefore, ENVI-met is considered the most suitable for this study after comparing the advantages and disadvantages of each model.

ENVI-met has been widely applied in simulating urban micrometeorological conditions such as dynamic surface temperature, solar radiation, heat flux from vegetation, and heat exchange inside water and soil; models from it have been validated against ground truth data [41, 42]. A simulated domain with a three-dimensional grid at 1 m resolution was created for each of the three neighborhoods. The ground-level vertical grid was further divided into five equidistant subgrids of 0.2 m for enhanced accuracy. A daily simulation was conducted for February 15, 2021, the day when the neighborhoods experienced the winter storm and power outages. The simulation covered 24 h, from 4:00 in the morning to 3:00 the next morning.

The prevailing meteorological input variables are summarized in Table 2, including air temperature, humidity, wind speed, wind direction; values were based on data collected by the Easterwood Field

Table 2

Prevailing meteorological parameters used as inputs to ENVI-met simulation.

| Parameter             | Value                 |
|-----------------------|-----------------------|
| Date                  | Feb 15/2021           |
| Duration (hrs)        | 24                    |
| Start time            | 4:00:00               |
| Wind speed (m/s)      | 6.48                  |
| Wind direction        | 327.5                 |
| Air temperature (°C)  | Min -12.2 to Max -6.7 |
| Relative humidity (%) | Min 61 to Max 84      |
| Sky condition         | Clear                 |

(KCLL) weather station, extracted from NOAA climate hourly data [57]. Input variables describing the natural and built environment consisted of soil type, ground surface pavement, building surface material, facade and roof greening, and vegetation. Details of the input parameters are listed in Appendix A (Table A1). The neighborhoods are relatively flat, with <5.0% slopes, and thus surface elevation was not considered. As there were no green walls or green roofs in these neighborhoods, there was no input data for building surface greening. Vegetation was modeled according to the species observed on-site, of which the most common were deciduous trees such as *Quercus virginiana* and *Lagerstroemia indica*; various conifers were also observed in Site III. Tree heights were estimated in meters using on-site measurements, and crown diameters were determined from satellite imagery [47]. Detailed plant model information is provided in Appendix A (Fig. A1). For boundary conditions, ENVI-met's simple forcing was used, which allows the input meteorological parameters to include diurnal variation.

### 2.4. ENVI-met model validation

Model validation and calibration was carried out using the above-mentioned *in-situ* micrometeorological data. ENVI-met models were constructed with the same natural and built environmental variables specified above, but a different set of meteorological data corresponding to the date/time of the field measurements acquired. Micrometeorological results for the measurement locations were extracted from the ENVI-met models and compared against the ground truth data. Model validity was determined according to the goodness of fit ( $R^2$ ) and root mean squared error (RMSE).

### 2.5. Biometeorological simulation

To estimate human thermal conditions during the winter storm from the micrometeorological results, we used two human energy balance models: the physiological equivalent temperature (PET) model [58] calculated in the ENVI-met BioMet module and the COMFA energy budget model calculated following the equation (2) [59]. The PET was widely accepted by previous studies to evaluate the outdoor micrometeorological conditions in both hot and colder zone [60]. And the result was interpreted as Celsius, which is easy to understand. COMFA gave a detailed calculation process, which can provide every part of energy fluxes that contribute to the total score. So COMFA is useful to detect how landscape elements may impact the components of the thermal comfort score.

The PET is defined as the physiological equivalent temperature at any given place (outdoors or indoors) and is equivalent to the air temperature at which, in a typical indoor setting, the heat balance of the human body (work metabolism 80 W of light activity, added to basic metabolism; heat resistance of clothing 0.9 Clo) is maintained with core and skin temperatures equal to those under the conditions being assessed [58]. And the PET is calculated based on the Munich energy balance model for individuals [58] as in Equation (1):

$$M + W + R + C + ED + ER_e + ES_w + S = 0 \quad (1)$$

where  $M$  is the metabolic rate,  $W$  is the physical work output,  $R$  is the net radiation of the body,  $C$  is the convective heat flow,  $E_D$  is the latent heat flow to evaporate water diffusing through the skin (imperceptible perspiration),  $E_{Re}$  is the sum of heat flows for heating and humidifying inspired air,  $E_{Sw}$  is the heat flow due to evaporation of sweat, and  $S$  is the storage heat flow for heating or cooling the body mass. The individual terms in this equation have positive signs if they result in an energy gain for the body and negative signs for an energy loss [58]. Meteorological parameters affect the individual heat flows in Equation (1) are as follows [58]:

- Air temperature:  $C, E_{Re}$

- Air humidity:  $E_D, E_{Re}, E_{Sw}$
- Wind velocity:  $C, E_{Sw}$
- Mean radiant temperature:  $R$

Human parameters included age, gender, weight, height, and clothing insulation (Table 3). As many residents suffer from financial difficulties and may lack winter clothing, we considered three different clothing heat resistance scenarios based on the types of clothing available and level of sedentary activity: the bare face Scenario 1, which simulated the condition with no clothing; the light clothing Scenario 2, which represented the individual as not having winter clothes and relying on pieces of summer clothes; and the warm clothing Scenario 3, which corresponded to the individual having sweaters or similar clothing pieces for cold weather in Texas. These clothing scenarios were developed based on results from a semi-structured interview about the adaptation strategies used by subsidized housing residents during the winter storm (Citation removed for double-blind review).

The COMFA model reports its result in terms of energy flux (W/m<sup>2</sup>) as a measurement of the total energy budget of a person, and further partitions the result into individual fluxes. Using both measures allowed us to identify which stream of energy is the most problematic, thus directing attention to the most effective interventions. The COMFA energy budget model was developed to incorporate human-environmental heat exchange and to consider microenvironmental effects on human thermal comfort. It is calculated using Equation (2):

$$\text{Budget} = M + \text{Rabs} - \text{Conv} - \text{Evap} - \text{Tremitted} \quad (2)$$

where  $M$  is the metabolic energy for heating the body (W/m<sup>2</sup>),  $Rabs$  is the absorbed solar and terrestrial radiation (W/m<sup>2</sup>),  $Conv$  is the sensible convective heat exchange (W/m<sup>2</sup>),  $Evap$  is the evaporative heat loss (W/m<sup>2</sup>), and  $TRemitted$  is the emitted terrestrial radiation (W/m<sup>2</sup>).

Input data for this model includes the air temperature (°C), wind speed (m/s), solar radiation (W/m<sup>2</sup>), relative humidity (%), solar elevation (degree), the solar transmissivity of objects between the person and the sun (%), clothing insulation conditions, and metabolism. The same set of biological parameters, including age, gender, weight, height, and clothing insulation, were used as inputs of the COMFA models (<https://research.ar.ch.tamu.edu/microclimatic-design/COMFA/index.html>). The raw output is a numeric value of energy flux measured in watts per square meter (W/m<sup>2</sup>) [59], and a lower value indicates more heat loss.

### 2.6. An environmental intervention for mitigating cold stress

Energy budget models provide output that identifies the thermal comfort level of a given location in the landscape, but they typically do not provide any advice or direction as to how thermally uncomfortable conditions could be improved. In this study we introduce an innovative way to use an energy budget model to identify the relative contribution of the various energy fluxes and to pinpoint those atmospheric variables that both can be readily modified by the design of the landscape and will have the largest positive effect in making conditions more thermally

**Table 3**  
Other parameters including clothing insulation scenarios used when calculating PET.

|                  | Scenario 1<br>(Bare face) | Scenario 2 (Light<br>clothing)                 | Scenario 3 (Warm<br>clothing)                                   |
|------------------|---------------------------|--|---|
| Clothing         | No clothing               | T-shirt, long pants, socks, shoes, windbreaker | T-shirt, long pants, socks, shoes, <i>sweater</i> , windbreaker |
| Insulation (clo) | 0                         | 0.72   | 1.07  |
| Age              | 35                        | 35   | 35  |
| Gender           | Male                      | Male   | Male  |
| Weight           | 75 kg                     | 75 kg  | 75 kg   |
| Height           | 1.75 m                    | 1.75 m   | 1.75 m  |

comfortable.

The COMFA model provides output that includes a quantitative value for each of the streams of energy (i.e.,  $M$ ,  $Rabs$ ,  $Conv$ ,  $Evap$ , and  $Tremitted$ ) as well as the atmospheric elements that affect each stream. Two components of human energy budget models are based on personal decisions and cannot be controlled by environmental interventions: metabolic energy and clothing level. Two other components, air temperature and air humidity, are typically spatially conservative at the micro-scale so they are less sensitive to small-scale landscape changes [51]. The elements that can be most readily modified by changes in the landscape are wind and solar radiation [51]. Wind is well-known to contribute substantially to the convective heat loss of people during cold weather [51]. During summer, solar radiation is often the largest contributor to the human energy budget and many studies have identified ways to reduce the amount of solar input that a person receives, but there are relatively few ways to safely increase the amount of solar radiation received in winter. Rather it is terrestrial radiation that has potential to provide increased heat flux to a cold person in winter.

We conducted a sensitivity analysis to examine the impacts of changes in each of the above-mentioned streams of energy in modifying thermal comfort. We modeled a person at locations D1 and compared the effects of raising air temperature of 3 °C, humidity of 10%, terrestrial radiation by increasing temperature of surrounding wall by 15 °C, and reducing wind speed by 50% and 75%. COMFA model was used to identify the relative effect of modifying different elements in the landscape. As expected, small variations in air temperature and air humidity had virtually no effect on the human energy budget. The effect of 3 °C air temperature reduced the convective heat loss by 12 W/m<sup>2</sup> and increased the  $Rabs$  by 11 W/m<sup>2</sup>. And the effect of 10% humidity reduction is also negligible (<1 W/m<sup>2</sup>). When the temperature of the wall was raised by 15 °C due to solar heating, the amount of terrestrial radiation emitted by the building was substantially increased. When the terrestrial radiation emitted by a cold wall (at air temperature) was replaced by the radiation from the wall that was warmed by solar radiation, but all other variables were kept constant, the effect was to increase the energy budget of a person standing at Location D1 by 15 W/m<sup>2</sup>. However, this effect diminished rapidly away from the building so that by position D5 the building added only 3 W/m<sup>2</sup> to the energy budget on the energy budget of a person. In comparison, the effect of reducing the wind by 50% reduced the energy lost through convection by 33 W/m<sup>2</sup>, and a 75% reduction in wind reduced the convective heat loss by 54 W/m<sup>2</sup>. This analysis pinpointed wind reduction as the most effective intervention to make the uncomfortably cold conditions more tolerable.

The literature [51,54–57] also confirmed that wind is a major factor influencing micro-scale variation in cold stress during extreme cold weather conditions. One previous study found that among several measured environmental factors pertaining to natural wind, wind velocity showed the highest correlation with subjects' comfort sensation votes [61]. Of several environmental modification strategies typically used for reducing wind velocity, windbreaks are among the most efficient [62], and the effective windbreak design in the literature typically consists of one or multiple rows of trees [63].

Tree configuration was decided based on previous studies [63–66], considering the number of rows, within row spacing, distance to buildings, orientation, and tree species:

- Number of rows: Kuhns and Brandle [63,64] suggested single-row windbreaks can be used where space is limited. In consideration of the subsidized housing community with limited space, the single-row format was selected.
- Within row spacing: Quam [65] suggested 1.8–6.1 m for conifers. While according to Kuhns [64], the within row spacing for larger evergreen trees can be 2.4–4.3 m. And it's recommended by Kuhns to avoid large gaps within the single row windbreaks [64]. Based on this information, the within-row spacing was 4 m in consideration of the tree type (conifers) and 5-m diameter of the tree canopy.

- Distance to building or protected area: Wright [66] indicated the greatest wind speed reduction occurs in the area from two times to ten times the height of the windbreak on the downwind side. In this study, we focused on the potential downwind wind speed change, so the distance between windbreak to D1-D5 should be within two times (30 m) to ten times (150 m) the heights, and it should not cross the neighborhood property boundary. Accordingly, the sample points' location (D1-D5) was 35–55 m away from the windbreaks.
- Orientation: The windbreaks are positioned at the upwind direction of the protected area [63]. The prevailing wind in January of College Station is North to West. During the winter storm period, the wind direction was 327.5°.
- Species: *Picea pungens* was chosen as the windbreak tree species for its ease of maintenance and tolerance of wind, flooding, and extremely low temperatures [67]. *Picea pungens* typically grows 10–18 m tall in cultivation; we chose 15 m as the tree height.

In summarize, as the subsidized apartment neighborhoods studied here have limited outdoor space and strong requirements for simultaneous improvement of microclimate conditions and outdoor space quality, tree rows (*Picea pungens*) were designed in the north and north-west directions as befit prevailing wind directions in the winter (Fig. 4). These windbreaks can protect the apartment buildings and associated outdoor environments from the cold winter wind. The tree rows were sited approximately 10–20 m away from buildings [64], and the within-row spacing was 4 m [64].

We further evaluated the impact of leaf area density on cold stress. Literature suggests that trees with crown LAD<sub>m</sub> values between 0.5 m<sup>2</sup>/m<sup>3</sup> and 1.5 m<sup>2</sup>/m<sup>3</sup> are generally considered sparse foliage, those with LAD<sub>m</sub> values close to 2.0 m<sup>2</sup>/m<sup>3</sup> have moderately dense foliage, and those with LAD<sub>m</sub> values higher than 2.5 m<sup>2</sup>/m<sup>3</sup> are considered dense [68]. Here, we assessed three windbreak tree density scenarios: very sparse (LAD<sub>m</sub> = 0.5 m<sup>2</sup>/m<sup>3</sup>), moderately sparse (LAD<sub>m</sub> = 1.0 m<sup>2</sup>/m<sup>3</sup>), and moderately dense (LAD<sub>m</sub> = 2.0 m<sup>2</sup>/m<sup>3</sup>).

Effectiveness of the intervention was assessed by comparing the Wind speed and PET between the pre-and post-values. Mean differences resulting from the intervention were statistically tested using paired-sample t-tests.

### 3. Results

#### 3.1. Model validation results

The ENVI-met model outputs, including air temperature and humidity, were validated against *in situ* measurements with agreement being examined in terms of the coefficient of determination (R<sup>2</sup>), which represents the proportion of the variation of the observed values (actual meteorological conditions) that is predicted by the simulated model predictions; and root mean square error (RMSE), which represents the normalized quantitative distance between the model predictions and the observed values (actual meteorological conditions). For air temperature, the predicted values demonstrated good agreement with measured

values (R<sup>2</sup> = 0.97, RMSE = 0.96, p < .001). For relative humidity, the agreement was slightly lower but still within a satisfactory range (R<sup>2</sup> = 0.85, RMSE = 3.53, p < .001). For air temperature, a review article [69] summarizing a total of 33 previous studies reported RMSE values between 0.4 and 3.9 °C, and the same review article reported R<sup>2</sup> values between 0.63 and 0.99. For the relative humidity, four previous studies reported RMSE between 2.7 and 13.0 and six studies reported the R<sup>2</sup> between 0.76 and 0.97 [69]. In summarize, the validation results of the study are satisfactory and generally consistent with prior studies of similar simulations.

#### 3.2. Micrometeorological conditions

The simulated micrometeorological results were reported at 1.5 m above ground to align with the human-meteorological reference height. Table 4 presents descriptive statistics for three time points: 7:00, 15:00, and 00:00; these represent the coolest daytime, the warmest daytime, and the coolest nighttime conditions on February 15.

During the winter storm, average air temperatures were far below the average for February; at night, the air temperature dropped to approximately −10 °C, then slowly raised to −7 °C in the afternoon. The monthly average temperature for February is over 17 °C higher, at 7 °C (1985–2015). Relative humidity ranged between 59.8% and 77.4%, similar to the documented monthly average (69.0%, 1985–2015). Wind speed was likewise near the monthly average (3 m/s, 1985–2015), but

**Table 4**

Means and standard deviations of simulated micrometeorological parameters for each site at three timepoints.

|                                     | Time  | Site I        | Site II       | Site III      | Diff.   |
|-------------------------------------|-------|---------------|---------------|---------------|---------|
| Air temperature (°C)                | 7:00  | -10.7 ± 0.2   | -10.4 ± 0.3   | -10.4 ± 0.2   | p < .01 |
|                                     | 15:00 | -8.1 ± 0.2    | -6.8 ± 0.2    | -6.9 ± 0.2    | p < .01 |
|                                     | 00:00 | -10.7 ± 0.2   | -10.6 ± 0.2   | -10.6 ± 0.2   | p < .01 |
| Relative humidity (%)               | 7:00  | 72.9 ± 0.5    | 70.6 ± 0.8    | 70.8 ± 0.7    | p < .01 |
|                                     | 15:00 | 62.7 ± 0.7    | 72.4 ± 2.5    | 70.2 ± 2.4    | p < .01 |
|                                     | 00:00 | 65.4 ± 0.2    | 63.8 ± 0.40   | 64.0 ± 0.4    | p < .01 |
| Wind speed (m/s)                    | 7:00  | 3.3 ± 0.9     | 2.7 ± 0.9     | 2.6 ± 1.0     | p < .01 |
|                                     | 15:00 | 3.6 ± 1.0     | 2.8 ± 1.0     | 2.6 ± 1.0     | p < .01 |
|                                     | 00:00 | 3.5 ± 0.9     | 2.7 ± 1.0     | 2.60 ± 1.0    | p < .01 |
| Solar radiation (W/m <sup>2</sup> ) | 7:00  | 0.0 ± 0.0     | 0.0 ± 0.0     | 0.0 ± 0.0     | p < .01 |
|                                     | 15:00 | 797.1 ± 271.7 | 858.3 ± 187.7 | 840.7 ± 208.0 | p < .01 |
|                                     | 00:00 | 0.0 ± 0.0     | 0.0 ± 0.0     | 0.0 ± 0.0     | p < .01 |

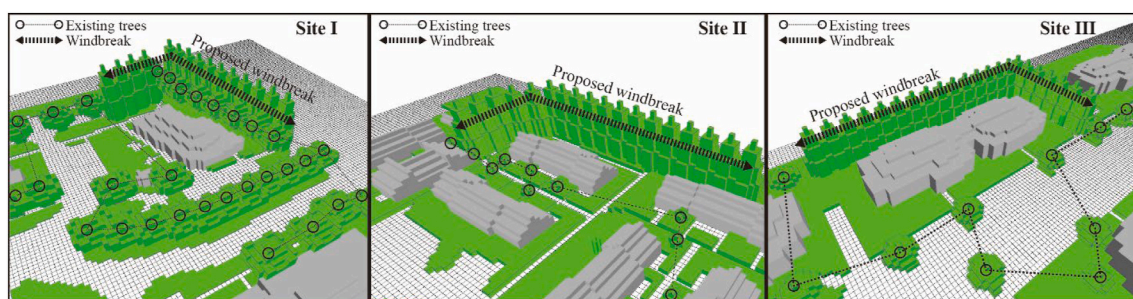


**Fig. 4.** Windbreak designs for each of the three sites (left to right: Site I, Site II, and Site III).

the standard deviation was approximately 1 m/s, indicating strong fluctuation. ANOVA tests suggested significant differences ( $p < .01$ ) in micrometeorological variables across the three sites, although difference was smaller for air temperature and relative humidity and larger for wind speed and solar radiation. For example, the average wind speed at 15:00 at Site I was 36.1% higher than that of Site III, and the mean direct shortwave radiation received by Site I was 5.5%–7.7% lower than those at Site II and Site III. These differences may be due to differences in tree canopy coverages, as Site I had the highest tree coverage ratio of 10.3%, versus 2.5% in Site II and 2.1% in Site III. Fig. 5 illustrates the inter- and intra-site variations in micrometeorological conditions.

### 3.3. Cold stress during the winter storm

The spatial and temporal dynamics of human cold stress in the built environment during the winter storm were evaluated from the PET and COMFA results. As clothing insulation is a major determiner of human heat flux in a given environment, we present results for two clothing conditions in Fig. 5: light clothes (insulation = 0.72) and warm clothes (insulation = 1.07). All three sites showed similar temporal trends relating to hourly solar elevation and direct solar radiation conditions. An initial low occurred at 7:00; then, PET and COMFA values increased during the day, finally peaking at 15:00. After 15:00, thermal values started to decrease, ultimately reaching a second low at midnight. In the light clothing scenario, initial values were very low (PET ~ -10.7 °C, COMFA ~ -253 W/m<sup>2</sup>), and thermal sensation as measured by the PET index consistently remained within the "extreme cold stress" range, except a few hours in the afternoon, when thermal sensation was classified as "strong cold stress." Wearing warm clothes seemed to be helpful in colder conditions: PET values were approximately two degrees

warmer versus the light clothes scenario. COMFA values indicated that cold stress was much more severe during the night, and wearing warm clothes could preserve heat by reducing a heat loss of more than 100 W/m<sup>2</sup>.

The thermal condition of the base point at 7:00 and 15:00 for each site is presented in Fig. 7. Strong spatial variations in thermal sensation of around 8 °C were observed within each neighborhood. Areas close to buildings were generally warmer, especially those within 10 m on the downwind side (5.0%–21.0% warmer than base point). As buildings could slow the wind, evaporative heat loss was suppressed in areas affected. Tree canopy and shading structures also impacted PET, but their effects varied with time; for example, in some locations, canopy cover rendered the area warmer at 7:00 but colder at 15:00. Before sunrise, solar radiation was not a major factor, and thus the reduced wind speeds under canopy cover contributed to greater PET values. In contrast, solar radiation was a major determinant of the thermal condition at 15:00, and reduction of solar radiation by canopy cover had a negative impact on PET values.

### 3.4. Buildings, wind, and cold stress

As the intra-neighborhood patterns indicated that the variations in wind speed and cold stress may be related to the presence and locations of buildings, we constructed COMFA models to represent a simplified typology comprising eight zones surrounding a building: upwind (U1), downwind (D1, D2, D3, D4, and D5), left-hand side (L1), and right-hand side (R1). The downwind area was divided into five zones due to that side featuring great gradients in thermal level. A base point was also included that is located away from the building in an open area.

Over the interval represented by D1 to D5, as distance to the building

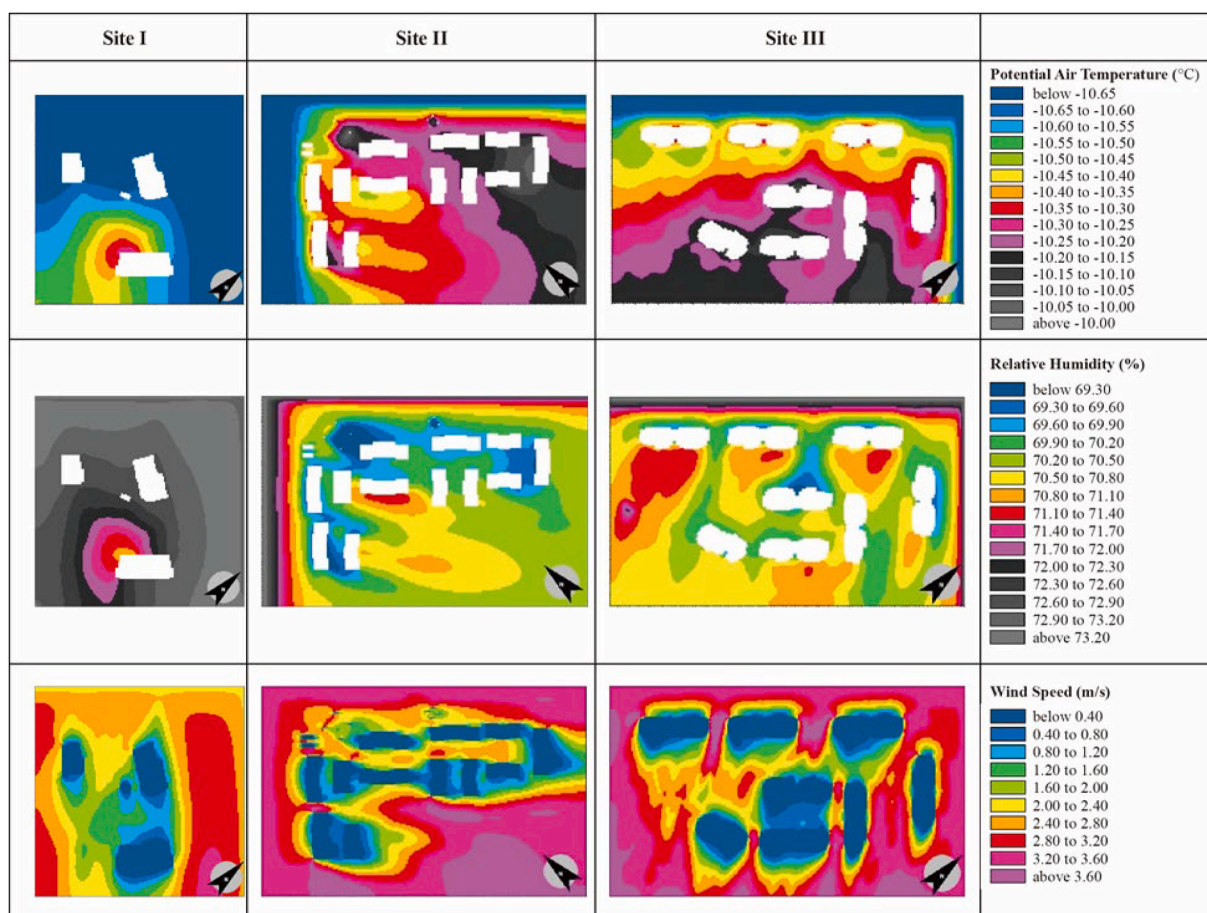


Fig. 5. Top view of spatial Patterns of air temperature, relative humidity, and wind speed at the three study sites (7:00).

façade increased, both PET and COMFA decreased (Fig. 8). At 7:00, there was no direct shortwave radiation and both relative humidity and air temperature were distributed evenly, thus wind speed change was the major factor impacting COMFA. It was observed that at 5 m from the building, the thermal sensation was warmer in both the upwind and downwind directions, suggesting the building to exert wind and cold mitigation effects. For the downwind direction in particular, those effects seemed to be nonlinear: PET and COMFA values dropped more steeply going from 5 to 10 m from the building, then the slope became gentler beyond 10 m.

### 3.5. Effects of windbreak designs in cold mitigation

To mitigate cold stress, windbreaks were proposed in the upwind direction where cold stress was more severe; three designs were considered, representing very sparse, moderate sparse, and moderately dense foliage conditions.

Fig. 9 shows the post-intervention increases in PET values (light clothing scenario). Table 5 presents the means and standard deviations of PET and wind speed values in areas near the building (area defined as up to 25 m in the downwind direction up to 10 m in other directions). Moderately dense foliage was found to be the most effective in reducing wind speed and improving thermal comfort, with mean wind speed being 20.4% to 41.1 lower—reduced by 0.7 m/s for Site I ( $p < .01$ ), 0.8 m/s for Site II ( $p < .010$ ), and 0.6 m/s for Site III ( $p < .01$ ). Thermal comfort conditions likewise improved under the moderately dense windbreak, with mean PET values increases of 1.4 °C for Site I ( $p < .01$ ), 2.6 °C for Site II ( $p < .01$ ) and 1.4 °C for Site III ( $p < .01$ ). In the moderately sparse scenario, average wind speed was reduced by 18.7% (Site I), 32.7% (Site II), and 20.9% (Site III), while average PET was improved by 1.0 °C (Site I), 2.0 °C (Site II), and 1.1 °C (Site III). The very sparse scenario only achieved an average wind reduction of 12.7% (Site I), 23.3% (Site II), and 14.7% (Site III), along with mean PET improvement of 0.7 °C (Site I), 1.5 °C (Site II), and 0.8 °C (Site III).

Regarding the locations that were most affected by the design intervention, more positive impact on thermal comfort was observed at U1, D1, and D2, while less impact was seen at D3, D4 and D5; this indicated the effect of the windbreak decreased with distance. Furthermore, although the windbreak’s effect extended behind a second wind-blocking structure, the effect ultimately wore off. Taking Site I as an example, the moderately dense windbreak had more apparent impact on cold stress at D1 ( $\Delta$ PET = 2.2 °C) and D2 ( $\Delta$ PET = 1.9 °C) compared with D3 ( $\Delta$ PET = 1.1 °C), D4 ( $\Delta$ PET = 0.5 °C), and D5 ( $\Delta$ PET = 0.1 °C) (Table 5). An exception was evident at D1 of Site II, where the moderately dense windbreak had less effect on both wind speed and thermal comfort ( $\Delta$ Wind speed = 0.05 m/s,  $\Delta$ PET = 0.26 °C) than either the very sparse ( $\Delta$ Wind speed = 0.08 m/s,  $\Delta$ PET = 0.30 °C) or moderately sparse ( $\Delta$ Wind speed = 0.08,  $\Delta$ PET = 0.40). A potential explanation is that D1 is located in a canyon created by the building; such areas have complex wind turbulence. The windbreak may disturb the flow field and alter the shape of horseshoe vortex, thus producing faster wind speeds and further lowering PET values. Another exception was observed at R1, for which Site III showed a much higher degree of wind speed reduction and

thermal improvement ( $\Delta$ Wind speed = 2.8 m/s,  $\Delta$ PET = 6.1 °C), relative to both Site I ( $\Delta$ Wind speed = 0.4 m/s,  $\Delta$ PET = 1.4 °C) and Site II ( $\Delta$ Wind speed = 1.6 m/s,  $\Delta$ PET = 2.8 °C). One potential explanation relates to the orientation of the buildings in the neighborhoods (Site I: 31° from north, Site II: 47° from north, Site III: 135° from north).

## 4. Discussion

This study investigated outdoor thermal comfort in three subsidized housing neighborhoods during the 2021 Winter Storm Uri. We used ENVI-met models to reconstruct microclimate conditions, employed two human thermal comfort indices to assess the degree of cold stress and its spatiotemporal patterns, and elucidated the effects of different clothing and windbreak scenarios in cold stress mitigation. In this section, we summarize the main results, discuss implications on policy and neighborhood design, and propose directions for future research.

### 4.1. Findings and contributions

The results of this study confirm that for both light and warm clothing scenarios (Fig. 6), the biometeorological cold stress during Winter Storm Uri was extreme for the majority of the day (remaining below 6 °C), but especially at nighttime (when it dropped to below 0 °C). For the light clothing scenario, extreme cold stress lasted about 13 h from 18:00 to 7:00 of the next day, the PET values were mostly between -10 °C and -8 °C. This diurnal variation was consistent with the result by Nastos [70], which indicated the extremely low PET between 0:00 to 7:00 and 18:00 to 24:00. COMFA values were mostly between -250 and -200W/m<sup>2</sup> (Fig. 6, Light clothing), which also indicated severe cold stress during nighttime. This result was consistent with Ziaul et al. [71] reported the slight cold stress during the daytime while strong cold stress during the nighttime and early morning in winter. This level of cold stress is dangerous and can lead to elevated risk of cold-related mortality for elderly adults if it persists for a prolonged time [72]. As many subsidized housing neighborhoods experienced power outages for several consecutive hours, indoor temperatures would continue to decrease until reaching levels similar to outdoor temperatures, leading to severe health consequences. The results also supported an important role for clothing insulation in keeping individuals warm during extreme cold stress (Fig. 6). With the Clo improving from 0.72 to 1.07, the COMFA values increased by an average of 105W/m<sup>2</sup> (Site I), 102W/m<sup>2</sup> (Site II), and 101W/m<sup>2</sup> (Site III), and the PET values increased by an average of 1.6 °C (Site I), 1.4 °C (Site II), and 1.4 °C (Site III), respectively. Those results were in line with the Andrade et al. [73] reported that more than 1.8 Clo was necessary during the winter night-time (PET < 4 °C). Those results present an additional inequality factor for low-income families in Texas, who may not be able to afford warm clothing or do not consider having backup clothing a priority over other basic needs.

Our study additionally demonstrated considerable spatial variation in biometeorological conditions due to the design characteristics of the neighborhoods. Not only was the level of cold stress different across the three neighborhoods, but it also greatly varies within each

**Table 5**  
Means and standard deviations of PET (light clothing scenario) and wind speed near the sample buildings under different windbreak foliage densities.

| Intervention scenarios |   | Site I       |                           | Site II      |                           | Site III     |                           |
|------------------------|---|--------------|---------------------------|--------------|---------------------------|--------------|---------------------------|
|                        |   | Mean ± 2Std. | Mean diff <i>p</i> -value | Mean ± 2Std. | Mean diff <i>p</i> -value | Mean ± 2Std. | Mean diff <i>p</i> -value |
| Wind speed (m/s)       | Original                                | 2.7 ± 1.7    |                           | 2.0 ± 1.1    |                           | 2.1 ± 1.9    |                           |
|                        | Scenario 1. Very sparse windbreak       | 2.3 ± 1.7    | <i>p</i> < .01            | 1.6 ± 1.1    | <i>p</i> < .01            | 1.8 ± 1.6    | <i>p</i> < .01            |
|                        | Scenario 2. Moderately sparse windbreak | 2.2 ± 1.8    | <i>p</i> < .01            | 1.4 ± 1.2    | <i>p</i> < .01            | 1.7 ± 1.4    | <i>p</i> < .01            |
|                        | Scenario 3. Moderately dense windbreak  | 2.0 ± 1.8    | <i>p</i> < .01            | 1.2 ± 1.2    | <i>p</i> < .01            | 1.5 ± 1.3    | <i>p</i> < .01            |
| PET (°C)               | Original                                | -9.7 ± 3.1   |                           | -8.5 ± 2.9   |                           | -8.4 ± 4.3   |                           |
|                        | Scenario 1. Very sparse windbreak       | -9.0 ± 3.4   | <i>p</i> < .01            | -7.0 ± 3.3   | <i>p</i> < .01            | -7.62 ± 3.8  | <i>p</i> < .01            |
|                        | Scenario 2. Moderately sparse windbreak | -8.6 ± 3.6   | <i>p</i> < .01            | -6.4 ± 3.6   | <i>p</i> < .01            | -7.3 ± 3.8   | <i>p</i> < .01            |
|                        | Scenario 3. Moderately dense windbreak  | -8.3 ± 4.0   | <i>p</i> < .01            | -5.9 ± 4.0   | <i>p</i> < .01            | -7.0 ± 3.9   | <i>p</i> < .01            |

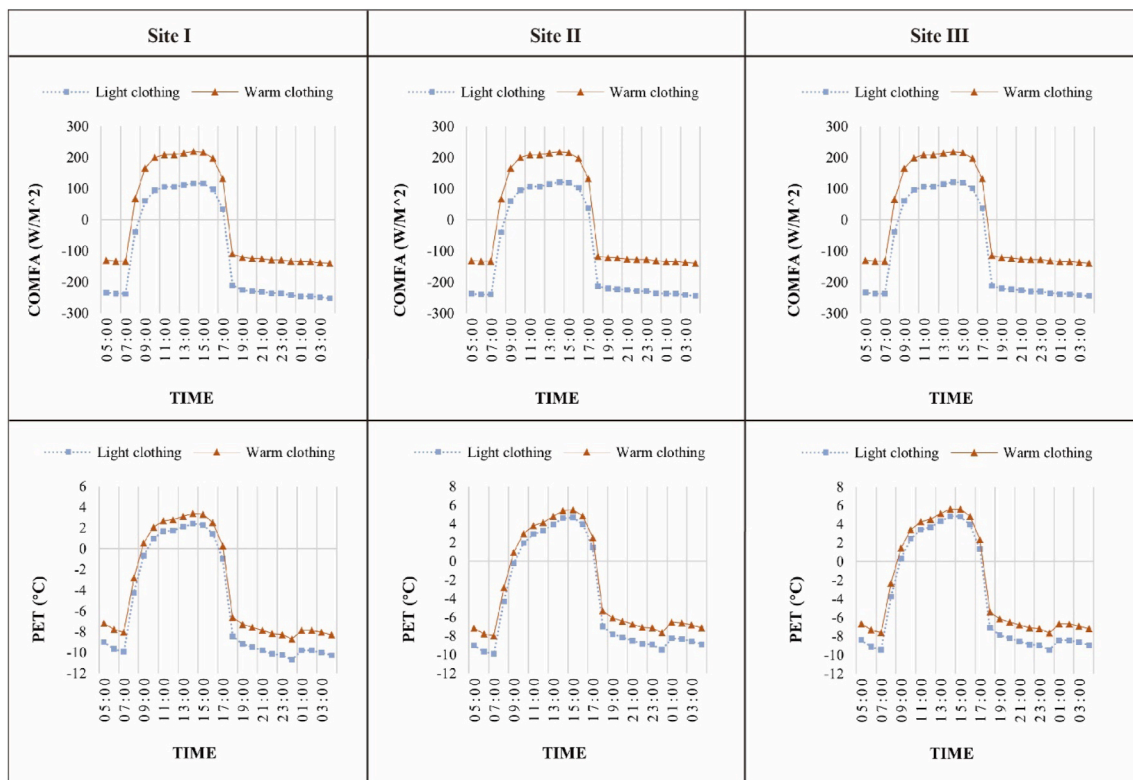


Fig. 6. Temporal Patterns of cold stress across the day as evaluated by PET and COMFA.

neighborhood because of the spatial typologies of buildings, pavilions, and tree canopy cover (Fig. 7). Tree canopy coverage played an important role in solar radiation and thermal comfort. Site I has 10.3% canopy coverage ratio, which is much higher than Site II (2.5%) and Site III (2.1%), the average direct shortwave radiation received at 15:00 was  $797.1 \pm 271.7 \text{ W/m}^2$  in site I, which was higher than site II ( $858.3 \pm 187.7$ ), and site III ( $840.7 \pm 208.0$ ). Table 5 shows that in the original scenario, Site I have a lower average PET of  $-9.0 \text{ }^\circ\text{C}$  compared with site II ( $-7.0 \text{ }^\circ\text{C}$ ), site III ( $-7.62 \text{ }^\circ\text{C}$ ). And this result is consistent with Teshnehdel et al. [74] reported the negative relationship between tree canopy coverage ratio and PET. Another example is the impact of wind on biometeorological conditions near the building, sophisticated patterns were evident in the meteorological conditions surrounding a building (Fig. 7). Both PET and COMFA indicated warmer thermal conditions surrounding areas on the upwind and downwind sides of the building. This result was consistent with Rui's study that reported warmer temperatures and lower wind speeds around the upwind and downwind sides [75]. It may be counterintuitive that both the upwind and downwind areas immediately around a building featured warmer thermal sensation compared to areas out in the open, although the spatial range of this protective effect was much extended in the downwind direction as intuitively expected. The impacts of canopy cover on thermal comfort were also complex and dependent on time of day because it can affect both wind pattern and solar radiation input. Solar radiation had a great impact on thermal comfort during the cold winter day, and thus the shade cast by tree canopies can exacerbate cold stress.

Mitigation designs such as windbreaks composed of trees are effective in reducing wind and consequently cold stress under extreme cold conditions, as the  $LAD_m$  increased from 0.5 to  $2.0 \text{ m}^2/\text{m}^3$ , the wind speed decreased, and the PET increased (Fig. 9). This result was consistent with Spangenberg et al. [76] that compared reported the trees with higher LAD have a higher effect in reducing the wind speed. Our study found that a single row of *Picea pungens* reduced wind speed by 2.45%–45.61% and increased thermal sensation by  $0.14 \text{ }^\circ\text{C}$ – $6.09 \text{ }^\circ\text{C}$  over a span of up to 40 m in the downwind direction (Fig. 9). Previous

evidence has shown trees and other plants to provide significant thermal improvement for urban environments in cold weather [77–79]. Our results further indicated that effect of the windbreak in reducing wind velocity was enhanced with denser foliage, which is consistent with findings from prior studies. For example, dense planting of evergreen trees is reported to block cold airflow more significantly, resulting in a greater improvement in PET and thus allowing a site to be more thermally comfortable [80].

#### 4.2. Policy and environmental design implications

This study calls policy attention to capacity building against extreme cold conditions in disadvantaged neighborhoods. As many subsidized housing projects in the United States were built in the 1960–1970s, their building layouts and environmental designs did not consider the extreme weather conditions and impacts associated with present-day and future climate change. Outdated infrastructure and thermal insulation often associate with unhealthy biometeorological conditions both outdoors and indoors. Even without power outages, energy burden and fuel poverty have been shown to relate to excess winter deaths in low-income neighborhoods [81]. When power outages occur, these residents, many of whom do not have a car or other means of transportation, are often stuck in their homes. Lack of warm clothing presents yet another layer of risk. Given these factors, environmental modifications that improve overall thermal performance and programs that provide necessities such as warm clothing during extreme weather conditions are essential. Assistance and programs providing on-bill financing, building retrofits that replace inefficient heating equipment, and better emergency warning systems may be helpful in preventing health risks.

Our study suggests that when planning and designing a neighborhood, the placing of structure and green infrastructure components should be carefully thought out based on thermal stress not only during summer but also the winter season. Our findings also reveal that building typology and the thermal conditions of the surrounding open space are closely related. The downwind area of buildings tends to have

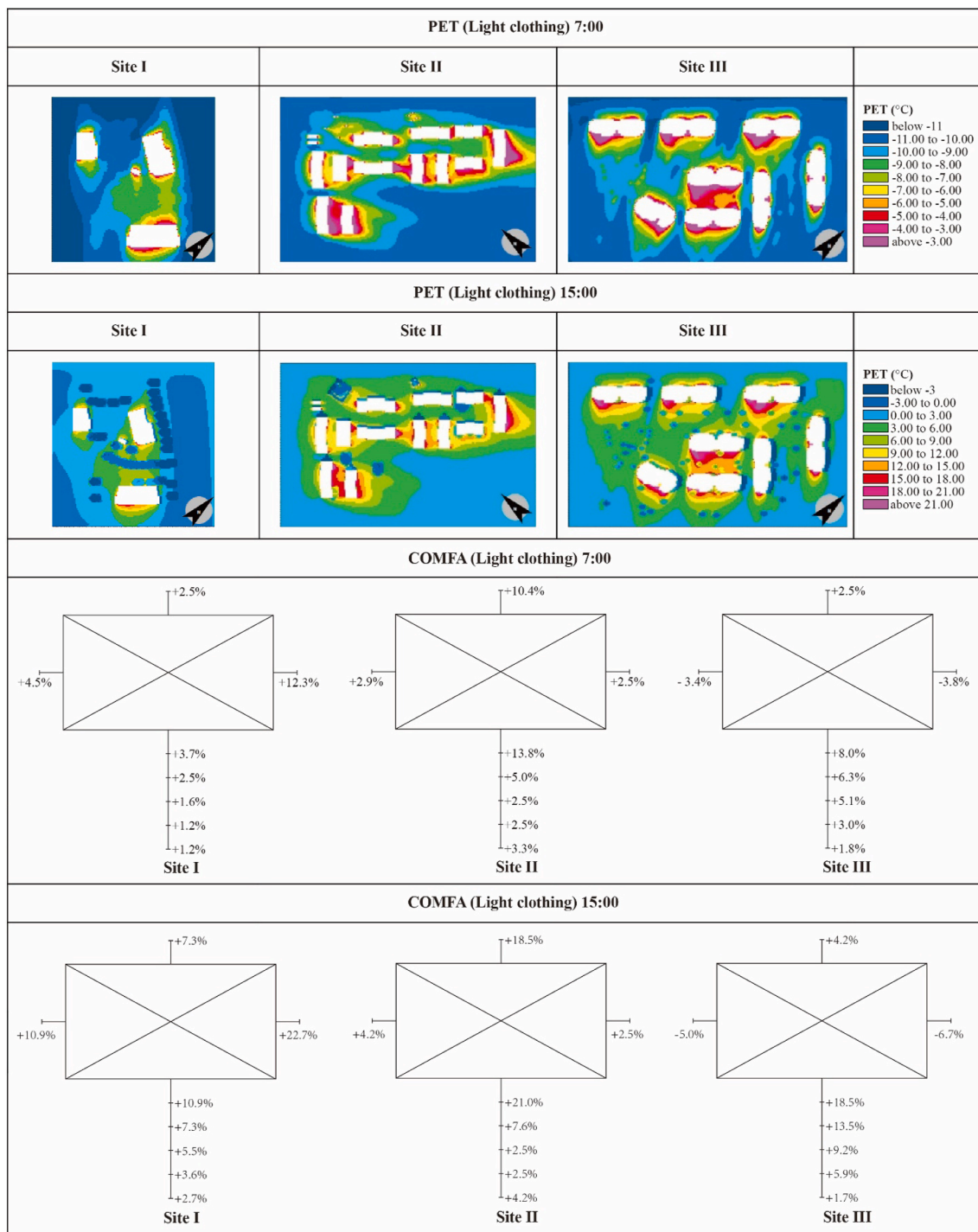


Fig. 7. Spatial variation in cold stress as evaluated by PET and COMFA.

warmer thermal comfort during cold weather; accordingly, policy-makers and designers should consider such downwind areas as spaces for outdoor activities during cold weather. Regarding vegetation, although evergreen species can improve shading and reduce radiation in the summer, excessive shading in the wrong location may exacerbate cold stress in the winter. Strategically located deciduous trees may be preferable, as they will provide shading in summer while also allowing solar radiation through in the winter. Windbreaks may be designed to mitigate cold stress in activity areas that are persistently colder or experience wind vortices.

This study also demonstrated significant temporal and diurnal

variations in cold stress, an important consideration as extra precautions are needed when cold stress is more severe. Air temperature alone would not reveal human thermal sensations or offer practical guidance on appropriate clothing to prevent cold stress. A warning system is needed to inform residents of the level of cold stress on an hourly basis and city block basis, and to give advice on appropriate clothing so residents can make informed decisions.

#### 4.3. Limitations and future study directions

Several limitations of this study need to be noted. First, as Winter

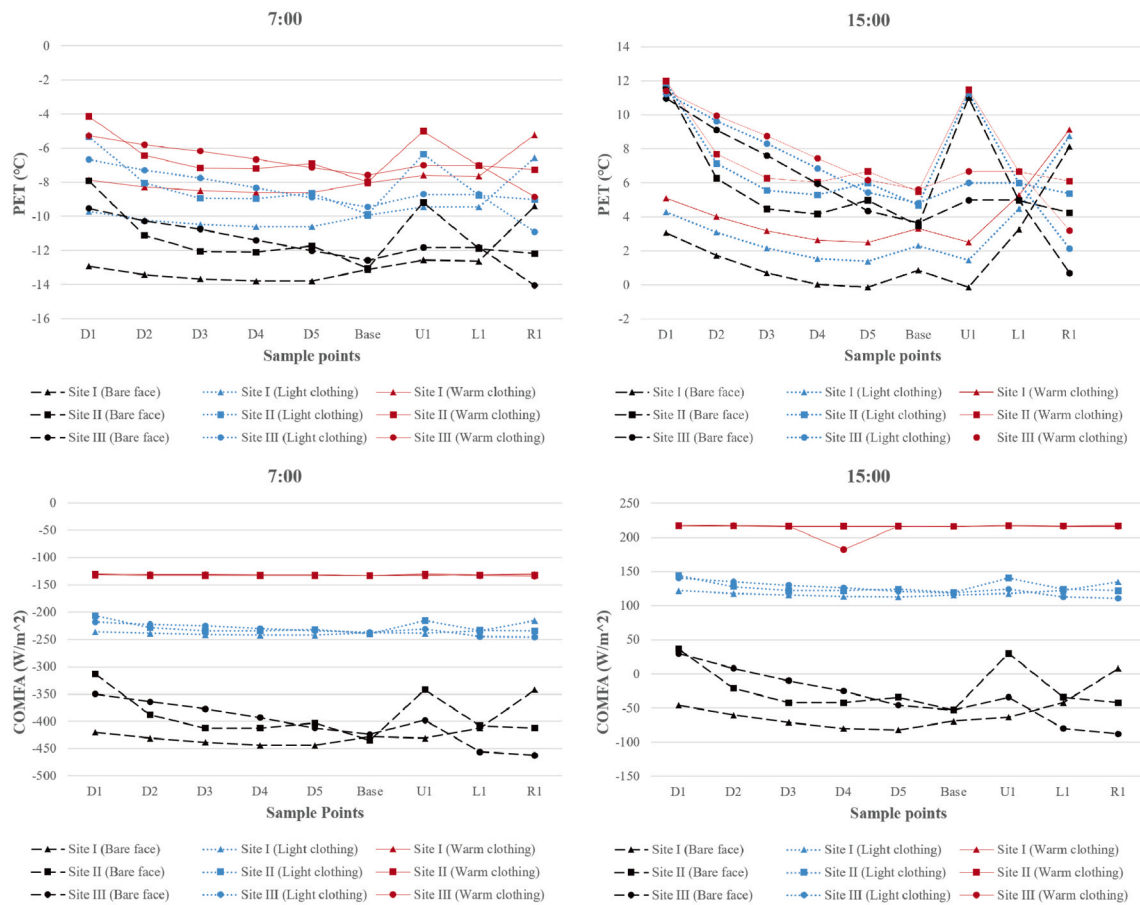


Fig. 8. Cold stress at selected sample points surrounding a building.

Storm Uri set record-low temperatures and crippled the infrastructure in Texas, we were unable to mobilize the team and make *in situ* measurements during the storm. Although field measurements were made under microclimates as closely-matching as possible and ENVI-met simulations of the day of the storm were utilized to reconstruct the conditions, the results cannot perfectly represent the actual cold stress experienced by residents. Future studies that aim at capturing extreme heat and cold conditions should develop emergency response plans to deploy teams into the field and use various portable and installed sensors to obtain microclimate data while those conditions are in effect. Our study also only considered three subsidized housing neighborhoods, which may not be representative of the full range of environmental and demographic conditions of such neighborhoods. This limitation may reduce the external validity of this study and the results should be discussed with caution when other settings are involved.

Methodologically, as our study focused on cold stress in the built environment, future studies can expand on this work by utilizing indoor thermal stress models to evaluate cold stress indoors, which may have stronger relationships with cold-related morbidity and mortality outcomes. Another important limitation is the short duration of the measurements made in each neighborhood (approximately 60 min) for the model validation. In order to compare the spatial distribution of microclimate conditions inter- and intra-neighborhoods and use research-grade microclimate measurements, we had to adopt the method of measuring multiple locations each during a short time. For example, research conducted by Zhao [82] used a vehicle equipped with sensors to do a short period traverse in the neighborhood. Jiang [83] use hand-held meteorological instruments to measure the meteorological situation of 10 sample points spread over the site (for the ENVI-met model calibration) at 10:00 a.m. Labdaoui [84] used the LM 8000 to

measure the microclimate of street at specific points in a short time to calibrate ENVI-met model. However, longer duration of measurement of at least 24 h would ensure that the diurnal conditions that affect solar radiation, shades, and wind can be accounted for. Future studies need to try to incorporate more complete hourly measurement and actual measured solar radiation or cloud conditions for better results in the numerical simulation. In addition, this study used the simple forcing mode of ENVI-met, which operates under a static cloud condition (clear sky) and so tends to overestimate solar radiation and underestimate cold stress.

Regarding the environmental intervention, this study mainly considered trees as the material for windbreaks; however, the contribution of such green infrastructure to a thermal environment depends on multiple factors including height, crown characteristics, vegetation coverage ratio, and planting arrangement. More complex planting arrangements and factorial designs that consider the interactions of these parameters on thermal performance would advance knowledge. The simplified typologies of vegetations used in this study are more effective in controlling for confounding factors and generating knowledge, but comprehensive designs for these neighborhoods should be considered to identify optimal scenarios for cold stress mitigation and better guide renovation practices. It is also necessary to identify designs that offer balanced thermal conditions throughout the year. In further studies, the thermal performance of proposed scenarios under both summertime and wintertime extreme weather conditions needs to be fully examined so as to develop integrated coping strategies for weather-related hazards.

## 5. Conclusion

Extreme weather conditions often place disproportionate burdens on

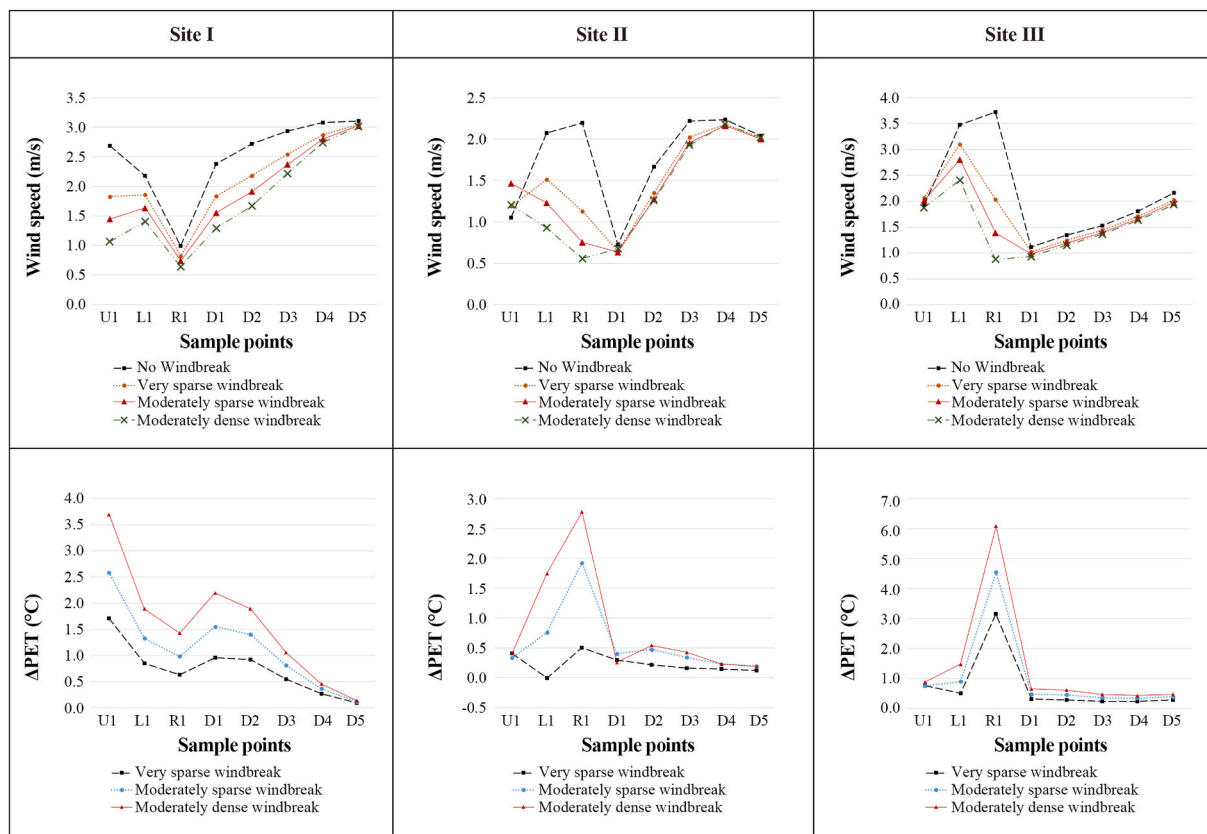


Fig. 9. Effect of windbreak foliage density on wind speed and cold mitigation (7:00).

disadvantaged communities such as subsidized housing neighborhoods. To our knowledge, our study is the first to examine cold stress in these neighborhoods during the record-setting 2021 Winter Storm and explore environmental modification methods for cold mitigation. Our results showed that the thermal conditions during the winter storm was assessed to be “extremely cold”, especially during nighttime. Not having warm clothes proved to be an additional risk factor associated with considerable decreases in human energy balance. By comparing simulations of windbreaks for cold mitigation, results showed the effects of moderately dense-foliage windbreak was the most effective in reducing wind speed and improving thermal comfort. Resources should be allocated to subsidized housing neighborhoods and environmental modification strategies should be considered increase community resilience to extreme temperature related hazards.

Appendix A

Table A1

Plans and the perspectives of ENVI-met models with detailed input parameters

|                   | Site I  | Site II  | Site III  |
|-------------------|---|--|---|
| Satellite imagery |  |  |  |

(continued on next page)

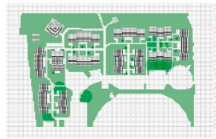
Funding

This work was supported by The Quick Response Research Award Program which is based on work supported by the National Science Foundation (NSF Award #1635593). Any opinions, findings, conclusions, or recommendations expressed in this material are those of the authors and do not necessarily reflect the views of the NSF or Natural Hazards Center.

Declaration of competing interest

The authors declare that they have no known competing financial interests or personal relationships that could have appeared to influence the work reported in this paper.

Table A1 (continued)

|                        | Site I  | Site II  | Site III  |
|------------------------|---|--|---|
| Model plan view        |  |  |  |
| 3D model               |  |  |  |
| Coordinates            | 30.61 N, -96.30W  | 30.61 N, -96.32W   | 30.68 N, -96.39W  |
| Rotation of grid north | -46°  | 46°  | -46°  |
| Soil type              | Default loamy soil  | Default loamy soil   | Default loamy soil  |
| Ground surface         | Grey concrete/asphalt road  | Grey concrete  | Grey concrete/deep water/asphalt road   |
| Building surface       | Default wall (moderate insulation)  | Default wall (moderate insulation)   | Default wall (moderate insulation)  |

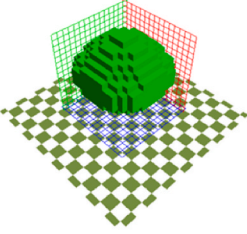
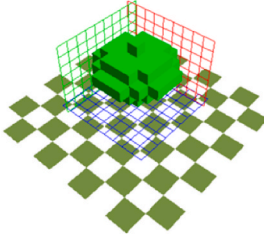
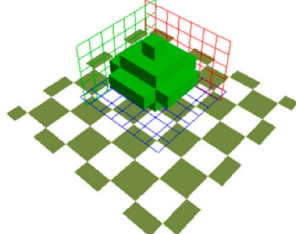
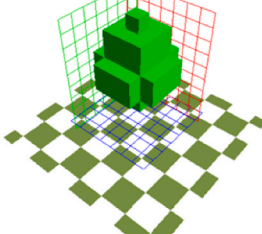
| Quercus Virginiana (1)   | Quercus Virginiana (2)   | Lagerstroemia indica   | Coniferous tree  |
|--|--|--|--|
|    |    |   |    |
| <p><b>General Information</b></p> <p>ID: 0LXY15 Color: <span style="background-color: black; color: black;">█</span></p> <p>Name: 13W15hi</p> <p>Alternative Name: <i>Albero nuovo</i></p> <p><b>Plant geometry</b></p> <p>Height (m): 15.00</p> <p>Width (m): 15.00</p> <p>Cells: 15 x 15 x 15</p> <p>Resolution (m): 1.00</p> <p><b>Basic properties</b></p> <p>CO2 fixation type: C3-Plant</p> <p>Leaf type: Deciduous Leafs</p> <p>Foliage Shortwave Albedo: 0.18</p> <p>Foliage Shortwave Transmittance: 0.30</p> <p><b>Advanced Properties</b></p> <p>Leaf Weight [g/m<sup>2</sup>]: 100.00</p> <p>Isoprene Capacity: 12.00</p> <p><b>Root Settings</b></p> <p>Depth of roots (m): 15.00</p> <p>Diameter of roots (m): 12.00</p> <p><input type="checkbox"/> Display Root Zone</p> | <p><b>General Information</b></p> <p>ID: H7W8ST Color: <span style="background-color: black; color: black;">█</span></p> <p>Name: H7W8ST</p> <p>Alternative Name: <i>Albero nuovo</i></p> <p><b>Plant geometry</b></p> <p>Height (m): 7.00</p> <p>Width (m): 9.00</p> <p>Cells: 9 x 9 x 7</p> <p>Resolution (m): 1.00</p> <p><b>Basic properties</b></p> <p>CO2 fixation type: C3-Plant</p> <p>Leaf type: Deciduous Leafs</p> <p>Foliage Shortwave Albedo: 0.18</p> <p>Foliage Shortwave Transmittance: 0.30</p> <p><b>Advanced Properties</b></p> <p>Leaf Weight [g/m<sup>2</sup>]: 100.00</p> <p>Isoprene Capacity: 12.00</p> <p><b>Root Settings</b></p> <p>Depth of roots (m): 4.00</p> <p>Diameter of roots (m): 7.00</p> <p><input type="checkbox"/> Display Root Zone</p> | <p><b>General Information</b></p> <p>ID: H5W6ST Color: <span style="background-color: black; color: black;">█</span></p> <p>Name: H5W6ST</p> <p>Alternative Name: <i>Albero nuovo</i></p> <p><b>Plant geometry</b></p> <p>Height (m): 5.00</p> <p>Width (m): 7.00</p> <p>Cells: 7 x 7 x 5</p> <p>Resolution (m): 1.00</p> <p><b>Basic properties</b></p> <p>CO2 fixation type: C3-Plant</p> <p>Leaf type: Deciduous Leafs</p> <p>Foliage Shortwave Albedo: 0.18</p> <p>Foliage Shortwave Transmittance: 0.30</p> <p><b>Advanced Properties</b></p> <p>Leaf Weight [g/m<sup>2</sup>]: 100.00</p> <p>Isoprene Capacity: 12.00</p> <p><b>Root Settings</b></p> <p>Depth of roots (m): 3.00</p> <p>Diameter of roots (m): 5.00</p> <p><input type="checkbox"/> Display Root Zone</p> | <p><b>General Information</b></p> <p>ID: H9W6CT Color: <span style="background-color: black; color: black;">█</span></p> <p>Name: H9W6CT</p> <p>Alternative Name: <i>Albero nuovo</i></p> <p><b>Plant geometry</b></p> <p>Height (m): 9.00</p> <p>Width (m): 7.00</p> <p>Cells: 7 x 7 x 9</p> <p>Resolution (m): 1.00</p> <p><b>Basic properties</b></p> <p>CO2 fixation type: C3-Plant</p> <p>Leaf type: Conifer Leafs</p> <p>Foliage Shortwave Albedo: 0.18</p> <p>Foliage Shortwave Transmittance: 0.30</p> <p><b>Advanced Properties</b></p> <p>Leaf Weight [g/m<sup>2</sup>]: 100.00</p> <p>Isoprene Capacity: 12.00</p> <p><b>Root Settings</b></p> <p>Depth of roots (m): 4.00</p> <p>Diameter of roots (m): 6.00</p> <p><input type="checkbox"/> Display Root Zone</p> |

Fig. A1. Detailed plants model setting in ENVI-met Albero.

## References

- [1] School of Public Affairs University of Houston, The Winter Storm of 2021, 2021.
- [2] Texas Department of State Health Services, Winter Storm-Related Deaths – July, vol. 13, 2021, p. 2021.
- [3] J. Stengle, M. Renault, Suspected hypothermia deaths in homes mount in Texas. 2021 May 20, Available from: <https://abcnews.go.com/US/wireStory/suspected-hypothermia-deaths-homes-mount-texas-76019295>, 2021.
- [4] W.B. Goggins, et al., Associations between mortality and meteorological and pollutant variables during the cool season in two Asian cities with sub-tropical climates: Hong Kong and Taipei, *Environ. Health* 12 (1) (2013) 1–10.
- [5] A. Sena, C. Corvalan, K. Ebi, Climate change, extreme weather and climate events, and health impacts, *Global Environmental Change. Handbook of Global Environmental Pollution* 1 (2014) 605–613.
- [6] W. Kirch, B. Menne, R. Bertollini, *Extreme Weather Events and Public Health Responses*, 2005.
- [7] F.C. Curriero, et al., Temperature and mortality in 11 cities of the eastern United States, *Am. J. Epidemiol.* 155 (1) (2002) 80–87.
- [8] A.J. McMichael, R.E. Woodruff, S. Hales, Climate change and human health: present and future risks, *Lancet* 367 (9513) (2006) 859–869.
- [9] S.L. Cutter, The changing nature of hazard and disaster risk in the Anthropocene, *Ann. Assoc. Am. Geogr.* 111 (3) (2021) 819–827.
- [10] J. Palm, K. Reindl, A. Ambrose, Understanding tenants' responses to energy efficiency renovations in public housing in Sweden: from the resigned to the demanding, *Energy Rep.* 6 (2020) 2619–2626.
- [11] S.L. Cutter, B.J. Boruff, W.L. Shirley, Social vulnerability to environmental hazards, *Soc. Sci. Q.* 84 (2) (2003) 242–261.
- [12] E. Ruel, et al., Is public housing the cause of poor health or a safety net for the unhealthy poor? *J. Urban Health* 87 (5) (2010) 827–838.
- [13] E.C. Digenis-Bury, et al., Use of a population-based survey to describe the health of Boston public housing residents, *Am. J. Publ. Health* 98 (1) (2008) 85–91.
- [14] I. Tsoulou, et al., Summertime Thermal Conditions and Senior Resident Behaviors in Public Housing: A Case Study in Elizabeth, vol. 168, *Building and Environment*, NJ, USA, 2020, p. 106411.
- [15] J. Huang, et al., Heat Stress and Outdoor Activities in Open Spaces of Public Housing Estates in Hong Kong: A Perspective of the Elderly Community, *Indoor and Built Environment*, 2020, 1420326X20950448.
- [16] K.K.-L. Lau, et al., The effect of urban geometry on mean radiant temperature under future climate change: a study of three European cities, *Int. J. Biometeorol.* 59 (7) (2015) 799–814.
- [17] E. Andreou, Thermal comfort in outdoor spaces and urban canyon microclimate, *Renew. Energy* 55 (2013) 182–188.
- [18] Á. Gulyás, J. Unger, A. Matzarakis, Assessment of the microclimatic and human comfort conditions in a complex urban environment: modelling and measurements, *Build. Environ.* 41 (12) (2006) 1713–1722.
- [19] E. Johansson, Influence of urban geometry on outdoor thermal comfort in a hot dry climate: a study in Fez, Morocco, *Build. Environ.* 41 (10) (2006) 1326–1338.
- [20] D. Lai, et al., Studies of outdoor thermal comfort in northern China, *Build. Environ.* 77 (2014) 110–118.
- [21] W. Yang, N.H. Wong, G. Zhang, A comparative analysis of human thermal conditions in outdoor urban spaces in the summer season in Singapore and Changsha, China, *Int. J. Biometeorol.* 57 (6) (2013) 895–907.
- [22] D. Lai, et al., Outdoor space quality: a field study in an urban residential community in central China, *Energy Build.* 68 (2014) 713–720.
- [23] J. Mi, et al., Outdoor thermal benchmarks and their application to climate-responsive designs of residential open spaces in a cold region of China, *Build. Environ.* 169 (2020) 106592.
- [24] A.A. Bakar, M.B. Gadi, Urban outdoor thermal comfort of the hot-humid region, in: *MATEC Web of Conferences*, EDP Sciences, 2016.
- [25] S. Oliveira, H. Andrade, An initial assessment of the bioclimatic comfort in an outdoor public space in Lisbon, *Int. J. Biometeorol.* 52 (1) (2007) 69–84.
- [26] T. Xi, et al., Influence of outdoor thermal environment on clothing and activity of tourists and local people in a severely cold climate city, *Build. Environ.* 173 (2020) 106757.
- [27] C. Piselli, et al., Outdoor comfort conditions in urban areas: on citizens' perspective about microclimate mitigation of urban transit areas, *Sustainable cities and society* 39 (2018) 16–36.
- [28] M. Nikolopoulou, S. Lykoudis, Thermal comfort in outdoor urban spaces: analysis across different European countries, *Build. Environ.* 41 (11) (2006) 1455–1470.
- [29] R.J. de Dear, K. Leow, S. Foo, Thermal comfort in the humid tropics: field experiments in air conditioned and naturally ventilated buildings in Singapore, *Int. J. Biometeorol.* 34 (4) (1991) 259–265.
- [30] N. Wong, et al., Thermal comfort evaluation of naturally ventilated public housing in Singapore, *Build. Environ.* 37 (12) (2002) 1267–1277.
- [31] M.B. Sosa, E.N. Correa, M.A. Cantón, Neighborhood designs for low-density social housing energy efficiency: case study of an arid city in Argentina, *Energy Build.* 168 (2018) 137–146.
- [32] H. Mahmoud, *Effect of urban form on outdoor thermal comfort of governmental residential buildings: New aswan as a case study, Egypt*. *JES, J. Eng. Sci.* 47 (3) (2019) 309–325.
- [33] B. Paramita, et al., Building configuration of low-cost apartments in Bandung—its contribution to the microclimate and outdoor thermal comfort, *Buildings* 8 (9) (2018) 123.
- [34] K.K.-L. Lau, S.C. Chung, C. Ren, Outdoor thermal comfort in different urban settings of sub-tropical high-density cities: an approach of adopting local climate zone (LCZ) classification, *Build. Environ.* 154 (2019) 227–238.
- [35] C. Gabbe, G. Pierce, Extreme heat vulnerability of subsidized housing residents in California, *Housing Policy Debate* 30 (5) (2020) 843–860.
- [36] L. Krebs, et al., Influence of extensive green roofs to the local microclimate: cooling assessment for a social housing project in the South of Brazil, *Proceedings of PLEA 2017 Edinburg: Design to thrive 2* (2017) 2880–2887.
- [37] P. Höppe, The physiological equivalent temperature—a universal index for the biometeorological assessment of the thermal environment, *Int. J. Biometeorol.* 43 (2) (1999) 71–75.
- [38] P.O. Fanger, *Thermal Comfort. Analysis And Applications in Environmental Engineering*. Thermal Comfort. Analysis and Applications in Environmental Engineering, 1970.
- [39] H. Mayer, P. Höppe, Thermal comfort of man in different urban environments, *Theor. Appl. Climatol.* 38 (1) (1987) 43–49.
- [40] J. Gaspari, K. Fabbri, M. Lucchi, The use of outdoor microclimate analysis to support decision making process: case study of Bufalini square in Cesena, *Sustainable Cities and Society* 42 (2018) 206–215.
- [41] J.A. Acero, K. Herranz-Pascual, A comparison of thermal comfort conditions in four urban spaces by means of measurements and modelling techniques, *Build. Environ.* 93 (2015) 245–257.
- [42] A. Ghaffarianhoseini, et al., Analyzing the thermal comfort conditions of outdoor spaces in a university campus in Kuala Lumpur, Malaysia, *Sci. Total Environ.* 666 (2019) 1327–1345.
- [43] S. Thorsson, M. Lindqvist, S. Lindqvist, Thermal bioclimatic conditions and patterns of behaviour in an urban park in Göteborg, Sweden, *Int. J. Biometeorol.* 48 (3) (2004) 149–156.
- [44] V. Cheng, et al., Outdoor thermal comfort study in a sub-tropical climate: a longitudinal study based in Hong Kong, *Int. J. Biometeorol.* 56 (1) (2012) 43–56.
- [45] T.-P. Lin, Thermal perception, adaptation and attendance in a public square in hot and humid regions, *Build. Environ.* 44 (10) (2009) 2017–2026.
- [46] M.W. Yahia, E. Johansson, Evaluating the behaviour of different thermal indices by investigating various outdoor urban environments in the hot dry city of Damascus, Syria, *Int. J. Biometeorol.* 57 (4) (2013) 615–630.
- [47] Z. Liu, et al., Heat Mitigation Benefits of Urban Green and Blue Infrastructures: A Systematic Review of Modeling Techniques, Validation and Scenario Simulation in ENVI-Met V4, *Building and Environment*, 2021, p. 107939.
- [48] M. Bruse, H. Fleer, Simulating surface-plant-air interactions inside urban environments with a three dimensional numerical model, *Environ. Model. Software* 13 (3–4) (1998) 373–384.
- [49] Y. Yang, et al., The “plant evaluation model” for the assessment of the impact of vegetation on outdoor microclimate in the urban environment, *Build. Environ.* 159 (2019) 106151.
- [50] M. Srivani, D. Jareemit, Modeling the influences of layouts of residential townhouses and tree-planting patterns on outdoor thermal comfort in Bangkok suburb, *Journal of Building Engineering* 30 (2020) 101262.
- [51] R.D. Brown, T.J. Gillespie, *Microclimatic Landscape Design: Creating Thermal Comfort and Energy Efficiency*, Wiley, 1995.
- [52] Gill-Instruments-Limited, *MaxiMet - user manual* [cited 2021 Nov. 11]; Available from: <http://gillinstruments.com/data/manuals/1957-PS-001%20Maximet%20Manual%20Issue%208%20for%20GMX%20100,%20200,%20300,%20301,%20400,%20500,%20501%20and%20600.pdf>, 2017.
- [53] H. Mittal, A. Sharma, A. Gairola, Numerical simulation of pedestrian level wind flow around buildings: effect of corner modification and orientation, *Journal of Building Engineering* 22 (2019) 314–326.
- [54] W.N. Hien, et al., Comparison of STEVE and ENVI-met as temperature prediction models for Singapore context, *International Journal of Sustainable Building Technology and Urban Development* 3 (3) (2012) 197–209.
- [55] K. Perini, et al., Modeling and simulating urban outdoor comfort: coupling ENVI-Met and TRNSYS by grasshopper, *Energy Build.* 152 (2017) 373–384.
- [56] L. Bande, et al., Validation of UWG and ENVI-met models in an Abu Dhabi District, based on site measurements, *Sustainability* 11 (16) (2019) 4378.
- [57] cited 2021 10, **May National Centers for Environmental Information, Local climatological data station details**, Available from, <https://www.ncdc.noaa.gov/cdo-web/datasets/LCD/stations/WBAN:03904/detail>.
- [58] P. Höppe, The physiological equivalent temperature – a universal index for the biometeorological assessment of the thermal environment, *Int. J. Biometeorol.* 43 (2) (1999) 71–75.
- [59] R.D. Brown, T.J. Gillespie, Estimating outdoor thermal comfort using a cylindrical radiation thermometer and an energy budget model, *Int. J. Biometeorol.* 30 (1) (1986) 43–52.
- [60] V.I. Part, *Environmental Meteorology, Methods for the Human-Biometeorological Evaluation of Climate and Air Quality for the Urban and Regional Planning at Regional Level. Part I: Climate*, VDI/DIN-Handbuch Reinhaltung der Luft, 2008, p. 29.
- [61] K.-N. Kang, D. Song, S. Schiavon, Correlations in thermal comfort and natural wind, *J. Therm. Biol.* 38 (7) (2013) 419–426.
- [62] R.D. Brown, *Design with Microclimate: the Secret to Comfortable Outdoor Space*, Island Press, 2010.
- [63] J.R. Brandle, D.L. Hintz, J. Sturrock, *Windbreak Technology*, Elsevier, 2012.
- [64] M.R. Kuhns, *Windbreak Benefits and Design*, 1998.
- [65] V. Quam, et al., Windbreaks for livestock operations, *Papers in Natural Resources* (1994) 123.
- [66] B. Wright, K. Stuhr, *Windbreaks: an Agroforestry Practice*, *Agroforestry Notes* (USDA-NAC), 2002, p. 25.
- [67] U.S.D.o. Agriculture, U.S. Science, E. Administration, *Agriculture Handbook*, U.S. Department of Agriculture, 1990.

- [68] S. Tsoka, T. Leduc, A. Rodler, Assessing the effects of urban street trees on building cooling energy needs: the role of foliage density and planting pattern, *Sustainable Cities and Society* 65 (2021) 102633.
- [69] C.K.C. Lam, et al., A review on the significance and perspective of the numerical simulations of outdoor thermal environment, *Sustainable Cities and Society* 71 (2021) 102971.
- [70] P.T. Nastos, I.D. Polychroni, Modeling and in situ measurements of biometeorological conditions in microenvironments within the Athens University Campus, Greece, *Int. J. Biometeorol.* 60 (10) (2016) 1463–1479.
- [71] S. Ziaul, S. Pal, Assessing outdoor thermal comfort of English Bazar Municipality and its surrounding, West Bengal, India, *Adv. Space Res.* 64 (3) (2019) 567–580.
- [72] R. Ruuhela, et al., Biometeorological assessment of mortality related to extreme temperatures in Helsinki region, Finland 1972–2014, *Int. J. Environ. Res. Publ. Health* 14 (8) (2017) 944.
- [73] H. Andrade, M.-J. Alcoforado, Microclimatic variation of thermal comfort in a district of Lisbon (Telheiras) at night, *Theor. Appl. Climatol.* 92 (3) (2008) 225–237.
- [74] S. Teshnehdel, et al., Effect of tree cover and tree species on microclimate and pedestrian comfort in a residential district in Iran, *Build. Environ.* 178 (2020) 106899.
- [75] L. Rui, et al., Study of the effect of green quantity and structure on thermal comfort and air quality in an urban-like residential district by ENVI-met modelling, *Building Simulation* 12 (2) (2019) 183–194.
- [76] J. Spangenberg, et al., *The Impact of Urban Vegetation on Microclimate in Hot Humid São Paulo*. Passive and Low Energy Architecture, 2007. Singapore.
- [77] S. Yilmaz, E. Mutlu, H. Yilmaz, Alternative scenarios for ecological urbanizations using ENVI-met model, *Environ. Sci. Pollut. Control Ser.* 25 (26) (2018) 26307–26321.
- [78] S. Yilmaz, et al., Analysis of Winter Thermal Comfort Conditions: Street Scenarios Using ENVI-Met Model, *Environmental Science and Pollution Research*, 2021, pp. 1–23.
- [79] S. Yilmaz, et al., Street design scenarios using vegetation for sustainable thermal comfort in Erzurum, Turkey, *Environ. Sci. Pollut. Control Ser.* 28 (3) (2021) 3672–3693.
- [80] L. Zhang, Q. Zhan, Y. Lan, Effects of the tree distribution and species on outdoor environment conditions in a hot summer and cold winter zone: a case study in Wuhan residential quarters, *Build. Environ.* 130 (2018) 27–39.
- [81] J. Teller-Elsberg, et al., Fuel poverty, excess winter deaths, and energy costs in Vermont: burdensome for whom? *Energy Pol.* 90 (2016) 81–91.
- [82] Q. Zhao, D.J. Sailor, E.A. Wentz, Impact of tree locations and arrangements on outdoor microclimates and human thermal comfort in an urban residential environment, *Urban For. Urban Green.* 32 (2018) 81–91.
- [83] Y. Jiang, et al., Microclimatic impact analysis of multi-dimensional indicators of streetscape fabric in the medium spatial zone, *Int. J. Environ. Res. Publ. Health* 16 (6) (2019).
- [84] K. Labdaoui, et al., The Street Walkability and Thermal Comfort Index (SWTCI): a new assessment tool combining street design measurements and thermal comfort, *Sci. Total Environ.* 795 (2021) 148663.